Supplement of Atmos. Chem. Phys. Discuss., 14, 19875–19915, 2014
http://www.atmos-chem-phys-discuss.net/14/19875/2014/
doi:10.5194/acpd-14-19875-2014-supplement

Atmospheric Chemistry and Physics Discussions

Supplement of

Investigating types and sources of organic aerosol in Rocky Mountain National Park using aerosol mass spectrometry

M. I. Schurman et al.

Correspondence to: M. I. Schurman (mishaschurman.ms@gmail.com)

S1. Supplement

S1.1 PMF Solution Diagnostics

Positive Matrix Factorization (PMF) is a positivity-constrained, receptor-only, least-squares regression algorithm used to deconvolve the matrix containing run-average (2-5 min) high-resolution organic mass spectra versus time into a chosen number of spectrally-static organic 'factors' whose contributions to total organic mass vary over time (Paatero 1997; Paatero & Tapper 1994). Spectral factors returned by PMF may be analyzed with meteorological data or anthropogenic inorganic tracers and compared to 'typical' spectra from various sources and/or degrees of processing to examine local chemistry (see main text); Ulbrich and coworkers have compiled an online database of AMS spectra spanning a broad range of sources, species, and sampling conditions (Ulbrich et al. 2009). Error and HR data matrix preparations followed Ulbrich et al. (2009). Isotopes were not included in the analysis, as their signal intensities are based on those of their parent ions and thus provide no additional chemical information.

The selection of number of PMF factors is based on factors' spectral and timeline dissimilarities (Figure S1(b)), comparison to 'established' factor types, and correlation with tracers (such as anthropogenic inorganic species concentrations) as is explored in the main text (Zhang et al. 2011; Ulbrich et al. 2012); factor number choice may be supported using Q (a parameter describing residuals) and other statistics. Q is defined as (Paatero et al. 2002):

$$Q = \sum_i \sum_j (e_{ij}/\sigma_{ij})^2$$

where e is residual not fit by the algorithm and σ is the estimated error over all rows (i, MS fragments) and columns (j, time) of the data and corresponding error matrices. For the Rocky Mountain study, a three-factor solution is supported by a large (36%) reduction in Q between two- and three-factor solutions, indicating that the three-factor solution describes considerably more of the variability in the dataset, but diminishing reduction (≤ 21%) in Q when 4 or more factors are chosen (Figure S1(c)). A second variable, Q_{exp}, equals the degrees of freedom (for AMS data, approximately the number of data points in the input data matrix) and $Q/Q_{exp} = 0.08$ for this dataset (Ulbrich et al. 2009; Paatero & Tapper 1993). As described in the literature, $Q/Q_{exp} << 1$ indicates an overestimation of error (Paatero et al. 2002; Ulbrich et al. 2009); we

hypothesized that the low total signal contributes to reduced signal-to-noise ratio overall, putting a larger percentage of data points (fragment mass at a given time) under the signal-to-noise (S:N = sqrt($\sum signal^2/\sum err^2$)) threshold that recommends down-weighting (increasing the error) during error matrix preparation; points with S:N<0.2 ("bad") are excluded from the analysis and those with 0.2<S:N<2 ("weak") are down-weighted by a factor of 2 (Paatero & Hopke 2003). All of the 'bad' fragments featured time series dominated by noise and thus their exclusion was sustained. The down-weighting factor for weak fragments was subsequently reduced to 1.2, resulting in $Q/Q_{exp} = 0.1$ for a three-factor solution. The Q/Q_{exp} improvement is minimal and the ensuing factors are nearly identical to those presented in Chapter 3, so the original analysis (down-weight factor of 2) was used. Although the source of the error overestimation was not determined, residual mass between measured values and the PMF reconstruction is low and fairly constant over time (Figure S1(f) and (g)); also, the histogram of scaled residuals for each m/z indicates that though the PMF reconstruction of mass tends slightly too low, this bias is consistent across m/z and thus should have little effect on the interpretation of results (Figure S1(d)).

The FPEAK parameter is used to explore linear transformations, or 'rotations,' of the PMF solution matrix that redistribute mass between the factor mass spectra and time lines while maintaining the positivity constraint (Ulbrich et al. 2009). FPEAK was varied from -1 to 1 (within which Q/Q_{exp} varied less than 10%; see Ulbrich et al., 2009), but none of these solutions improved description of the aerosol characteristics at the Rocky Mountain site. Thus, FPEAK = 0 was selected for Rocky Mountain; RotMat, which describes the rotational freedom of the solution, or number of possible MS-time series combinations, is also minimized with FPEAK=0 as recommended by Paatero and Hopke (2003) and others (Lanz et al. 2007). The Rocky Mountain PMF analysis was repeated twice from HR fragment selection onward and twice with different error constraints with very similar results.

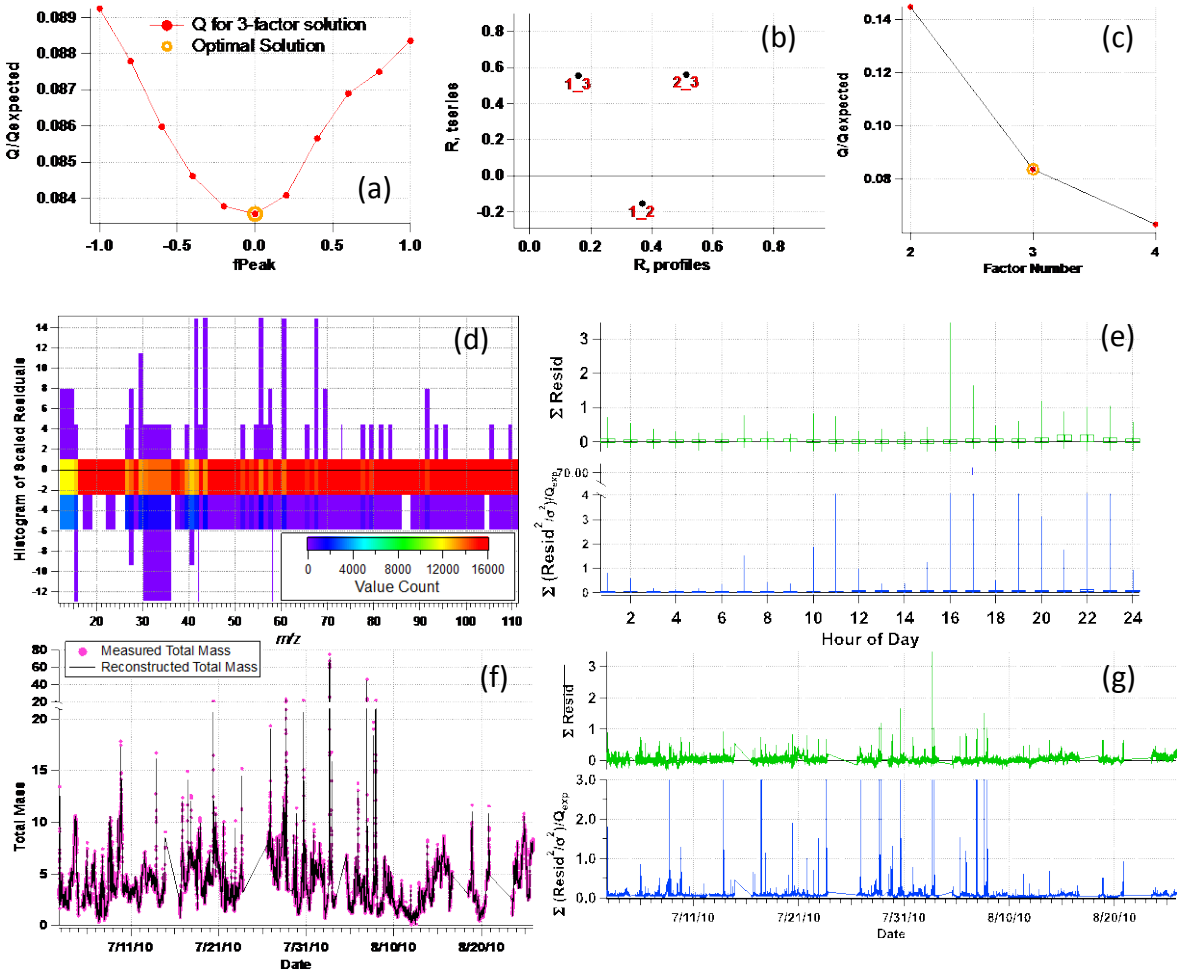

Figure S1: Diagnostic plots for the optimal 3-factor PMF solution explored in the main text. (a) Q/Q_{exp} for varying FPEAK values for a 3-factor solution, (b) Pearson's correlation coefficients between factor time series and mass spectral profiles, where Factor 1 = BBOA, Factor 2 = LV-OOA, and Factor 3 = SV-OOA, (c) Q/Q_{exp} for various numbers of factors, (d) histogram of scaled residuals for each *m/z* (Scaled residual = (measured-reconstructed)/measured), (e) hourly diurnal (top) sum of residuals and (bottom) Q/Q_{exp} (boxes are the mean; whiskers 25th and 75th percentiles), (f) total measured and reconstructed mass, and (g) sum of residuals (top) and Q/Q_{exp} (bottom) over time.

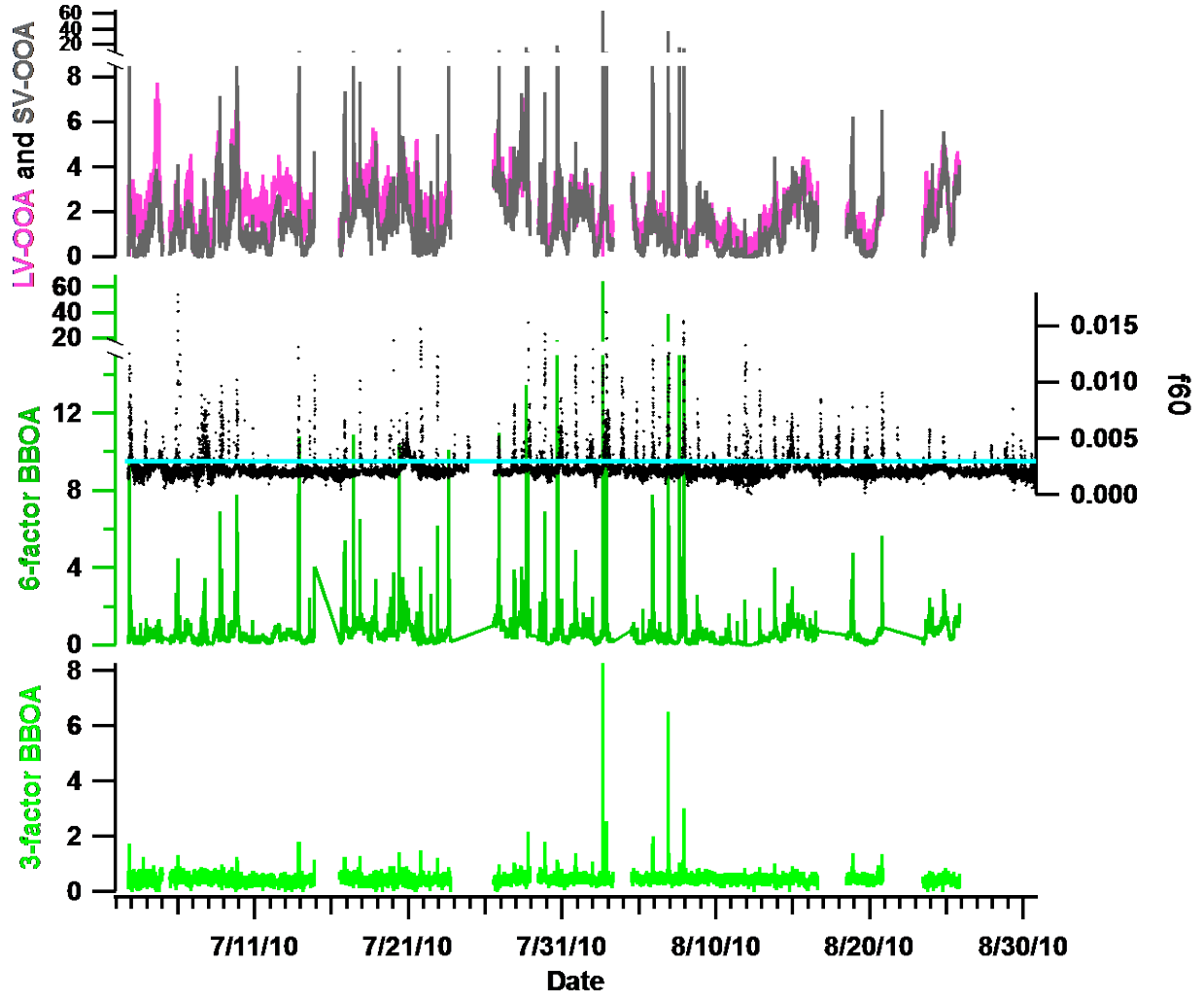

Figure S2: Timelines of LV-OOA, SV-OOA, and BBOA from the 3-factor PMF solution, BBOA from a 6-factor recombination, and *f*60 (the light blue line on right axis shows the ambient *f*60 background value (0.003), above which biomass burning is indicated).

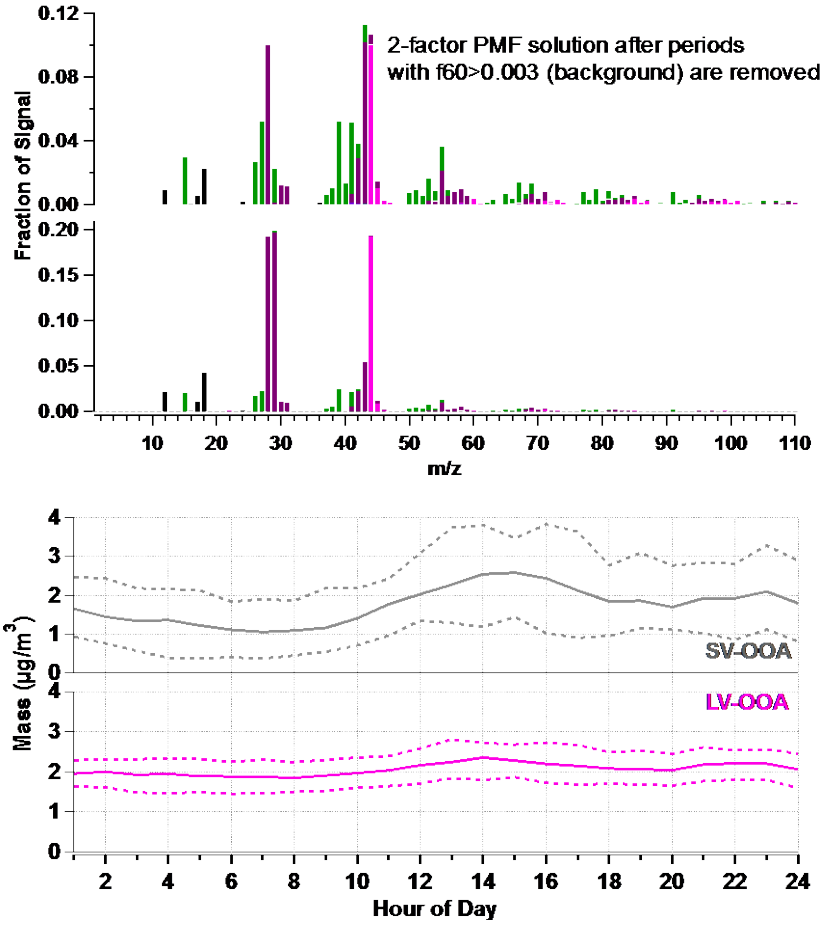

Figure S3: (top) Mass spectra and (bottom) diurnal hourly averages of factors from a PMF analysis omitting periods with elevated *f*60 (*f*60 > 0.003, the ambient background value).

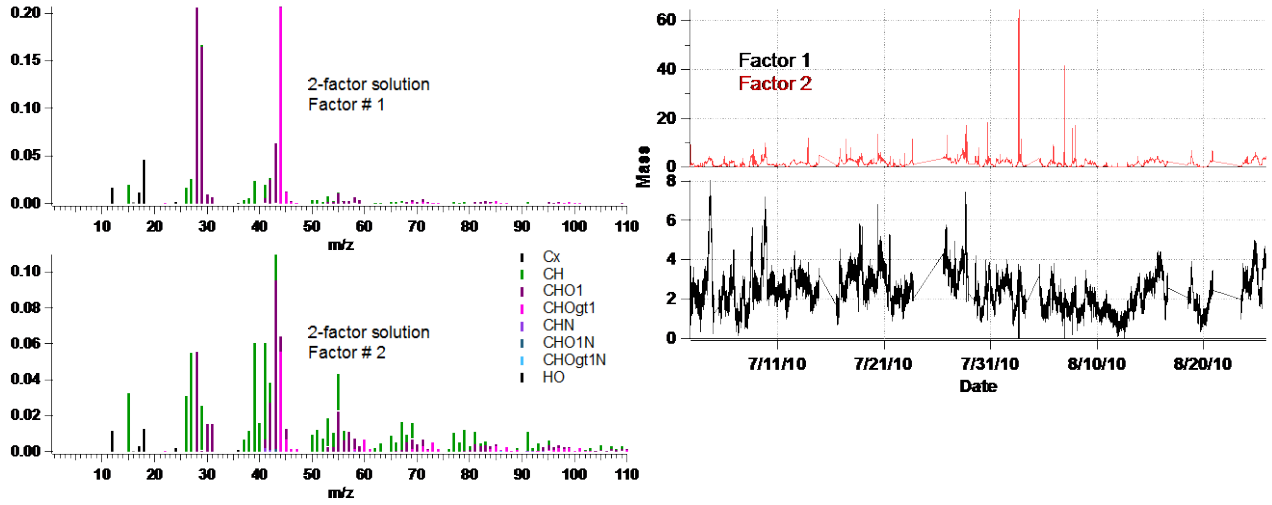

Figure S4: A 2-factor PMF solution of the high-resolution organic matrix: (left) factor mass spectra colored by fragment family signal contributions, and (right) time series of each factor.

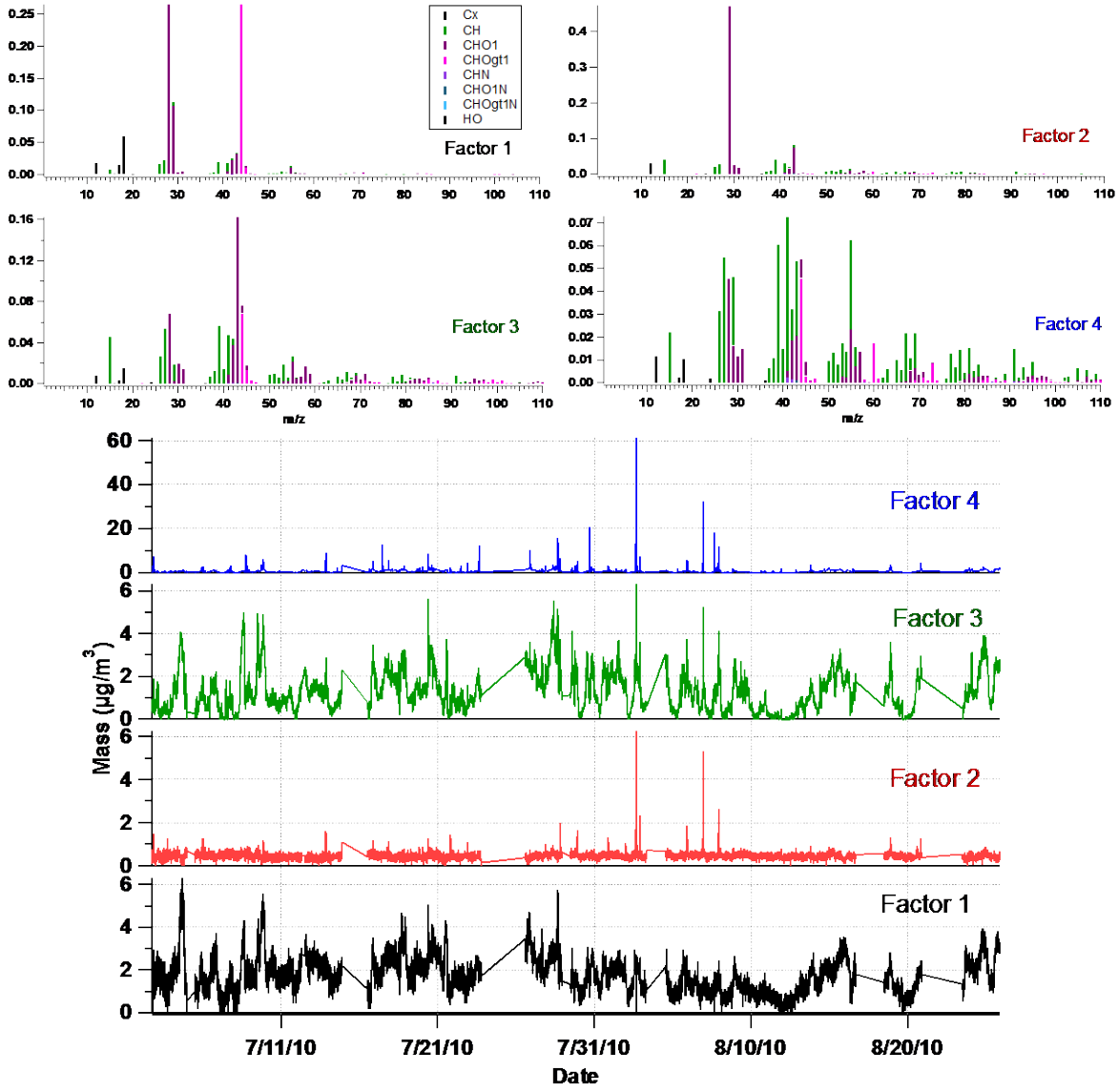

Figure S5: A 4-factor PMF solution of the high-resolution organic matrix: (top) factor mass spectra colored by fragment family signal contributions, and (bottom) time series of each factor.

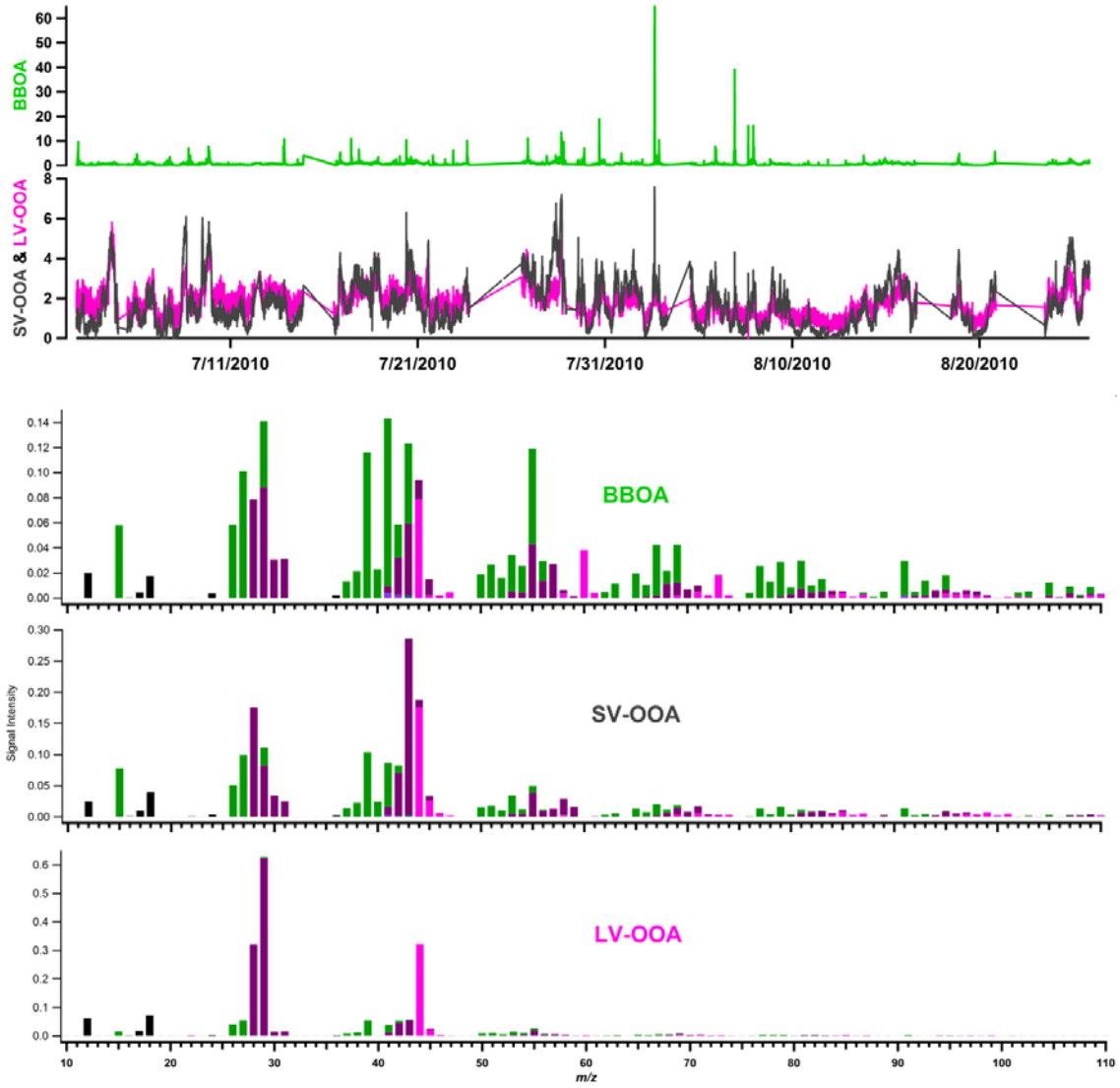

Figure S6. Timelines and mass spectra from PMF six-factor recombination of the Rocky Mountain dataset.

Table S1. Time-series correlations between inorganic species and organic factors from recombination of factors in a six-factor analysis (IGOR linear regression).

Timeline Correlation (r^2)	LVOOA	SVOOA	BBOA
SO_4	0.43	0.29	0.02
NO_3	0.31	0.32	0.07
NH_4	0.49	0.34	0.03

S1.2 Elemental Analysis:

Slopes during periods dominated by each factor are all close to -0.5 (m_{LV} = -0.54; m_{SV} = -0.56; m_{BB} = -0.53), consistent with other ambient aerosol studies (Ng et al. 2011). The photo-oxidation of α-pinene also produces this slope, consistent with possible biogenic contributions, although other reactions can of course yield similar slopes (Chhabra et al. 2011; Lambe et al. 2011); also, because the air masses herein are not isolated, it is also possible that transportcould be influencing the observed changes in van Krevelen space in place of or addition to in-situ reaction.

S1.3 Estimation of PToF Sizing Error:

PToF sizing error should not be confused with PToF mass error calculations in Ulbrich et al. (2012). Sources of error in PToF size determination include, but are not limited to, 'chopper broadening' caused by the spread in particle arrival times caused by the time it takes the chopper slit to pass through beam (particles at end of transmission time enter flight slightly later than ones at beginning); since differently sized particles fly at different velocities, this error is size dependent (Allan et al., 2003). For a 1% chopper at 150Hz, the amount of time that the chopper is open, which influences the spread of the sized particles arriving at the vaporizer, can be calculated by:

$$\left(\frac{6.7\ \text{ms}}{\text{revolution}}\right)\left(\frac{0.01\ \text{open chopper}}{\text{revolution}}\right)\left(\frac{\text{revolution}}{2\text{x}0.5\%\ \text{slits}}\right) = 0.034\frac{\text{ms}}{\text{revolution}} \quad \text{(Equation 1)}$$

For each particle size, the chopper transmission time can be compared to total particle flight time to determine chopper-broadening error. The particle PToF flight time can be calculated via:

$$\text{Velocity} = p_3 + \frac{(p_0 - p_3)}{(1+(D_{va}/p_1)^{p_2})} \quad \text{(Equation 2)}$$

where p_0 = velocity of the gas after the aerodynamic lens, p_1 = D*(nm) coefficient, p_2 = b coefficient, p_3 = velocity of the gas in the aerodynamic lens (determined during the size calibration). For example, using size calibration values for the study presented herein, a 300 nm-particle flight time of 0.003136 seconds yields an error of 0.000034 s/0.003136 s = 0.011 or 1.1%.

Chopper broadening error is exacerbated by error in PSL or DMA-selected ammonium nitrate used for sizing (error about the size calibration curve); since these errors have different units, each is calculated as a percentage of diameter at each given size and compounded via:

$$\text{Total Error (\% of diameter)} = \sqrt{\sum_i e_i^2} \qquad \text{(Equation 3)}$$

where e is the % error for each relevant process. Polystyrene latex spheres (PSL, Duke Scientific Corp.) are used for size calibration points at 70, 100, 200, 300, 400, 500, and 700 nm, and have precisions of 1.5-9 nm, depending on size. For example, 300nm PSL particles have a diameter standard deviation of 5 nm or 0.0167 (1.7%) of particle size. Compounding chopper broadening and calibration errors yields a total 2.7% error in size determination for 300 nm particles during this study; these calculations were iterated at the diameters listed above for each field experiment. Other possible PToF errors and caveats to a complete PToF error determination are outlined in Ulbrich et al. (2012). The PToF size resolution is 5-10 $D_{aero}/\Delta D_{aero}$ (FWHM) over the size range of aerodynamic lens transmission (Aerodyne Research Inc. 2004).